

Decatungstate-Photocatalyzed Acylation of Single-Walled Carbon Nanotubes

Ruben Canton-Vitoria, Mildred Quintana, Nikitas G. Malliaros, and Nikos Tagmatarchis*

Although the functionalization and modification of single-walled carbon nanotubes (SWCNTs) has been advanced for two decades, their chemical transformation via catalytic processes has yet to be explored and further facilitate their industrial utility. Here, the decatungstate-photocatalyzed acylation is described of semiconducting (7,6)SWCNTs and the scope of the reaction is investigated by employing alkyl, aromatic, and organometallic aldehydes. The success of the methodology is confirmed by diverse spectroscopic, thermal, microscopy imaging, and redox techniques. The developed catalytic process for the functionalization of SWCNTs is environment friendly, since the catalyst and unreacted aldehydes can be recovered and reused, while the modified SWCNTs can be easily isolated and purified by membrane filtration. It is believed that the current findings will open new avenues for the catalytic functionalization of SWCNTs and the approach is intended to extend for modifying 2D nanomaterials.

The next important challenge in the functionalization of SWCNTs is to develop chemical transformations based on catalytic processes. Among other advantages, catalytic processes are particularly attractive in industry, with benefits directly related with the development of large-scale modified SWCNTs for various purposes and technological applications.

In general, catalysis in chemical transformations not only avoids the formation of byproducts but most importantly accelerates reaction rate and often plays major role in atom economy, without generating waste. This is something yet to be realized in SWCNTs modification strategies, namely to develop a catalytic route in which all atoms from the starting

materials are present in the product. In this context, a polyoxometalate complex $W_{10}O_{32}^{4-}$, consisting of 10 W atoms and 32 O atoms, with a charge of -4 and *n*-tetrabutylammonium counter cation, namely tetrabutylammonium decatungstate (TBADT), with interesting photochemical and photophysical properties, has its own share in catalysis.^[8] Briefly, in TBADT complex, the alkyl chains of tetrabutylammonium cation enhance solubility in organic media, while $W_{10}O_{32}^{4-}$ is directly responsible for the catalytic activity. Hence, upon photoexcitation an electron from the 2p orbital of O moves to the empty 5d orbital of W, leaving behind a hole at O, in a ligand-to-metal charge-transfer, LMCT, process. The LMCT transforms to a longer-lived and more stable intermediate wO , which is responsible for the oxidation of organic substrates, yielding the reduced form of $W_{10}O_{32}^{5-}$.^[9,10] Please note that this wO is not derived by the reduction of W, but rather from the delocalization of the photoexcited electron in every atom of the complex.


While TBADT has been widely investigated as photocatalyst for the oxidation of organic substrates under aerobic conditions, its anaerobic utility for C–C bond formation via C–H bond fragmentation has been less screened.^[8] The catalytic activity of TBADT, once photoexcited, regards its deep highest occupied molecular orbital (HOMO) at -7.13 eV, which is able to accept hydrogen atoms even from light alkanes, e.g., methane with hydrogen atom dissociation energy 4.55 eV,^[11] thus being extremely easy to occur for other organic moieties such as aldehydes.^[12] Notably, a few monoadducts of C_{60} derived by radical addition of substituted toluenes and anisoles,^[13] aldehydes,^[14] ethers,^[15] alcohols,^[16] and lactones^[17] with TBADT as photocatalyst have been reported. In the decatungstate-photocatalyzed acylation of C_{60} , the HOMO and lowest unoccupied molecular orbital energy levels of C_{60} (-5.87 and -4.18 eV, respectively)^[18]

1. Introduction

Single walled carbon nanotubes (SWCNTs) are 1D materials with a bandgap at the near-IR region of the electromagnetic spectrum and show carrier mobility superior of $1000 \text{ cm}^2 \text{ V}^{-1} \text{ s}^{-1}$. These excellent properties make SWCNTs potential candidates in different nanotechnology areas.^[1–4] Chemical functionalization, on the other hand, is a powerful technique to expand or tune SWCNTs properties.^[5] Basically, SWCNTs have inferior chemical reactivity compared to fullerenes,^[6,7] which makes them chemically stable enough, at least not to get oxidized at room temperature. However, SWCNTs can react with organic species forming robust and stable covalent bonds, with the particular field of research to blossom during the last two decades, resulting in the construction of a plethora of modified SWCNTs featuring diverse chemical species onto their framework.^[6,7]

R. Canton-Vitoria, N. G. Malliaros, N. Tagmatarchis
Theoretical and Physical Chemistry Institute
National Hellenic Research Foundation
48 Vassileos Constantinou Avenue, Athens 11635, Greece
E-mail: tagmatar@eie.gr

M. Quintana
High Resolution Microscopy-CICSaB and Faculty of Science
Universidad Autónoma de San Luis Potosí
Av. Sierra Leona 550, Lomas de San Luis Potosí, SLP 78210, Mexico

 The ORCID identification number(s) for the author(s) of this article can be found under <https://doi.org/10.1002/admi.202201575>.

© 2022 The Authors. Advanced Materials Interfaces published by Wiley-VCH GmbH. This is an open access article under the terms of the Creative Commons Attribution License, which permits use, distribution and reproduction in any medium, provided the original work is properly cited.

DOI: 10.1002/admi.202201575

are properly aligned with those of TBADT and TBADT⁻H⁺ (−7.13 and −3.48 eV, respectively),^[19] energetically driving the reaction. Considering that the valence and conduction band of semiconducting SWCNTs lie in similar energies with the aforementioned of C₆₀ (−4.90 and −3.88 eV, respectively),^[20] analogous placement with TBADT and TBADT⁻H⁺ occurs. Screening the bibliography, only a preliminary study of TBADT with carbon nanotubes and polyethylene glycol (PEG) was found.^[21] However, PEG could react upon activation of either the primary carbon of the alcohol or the secondary carbon of the ether unit, resulting in an indistinguishable chemical process between nanotubes and polymer, preventing clear understanding and subsequent exploitation of TBADT in the modification of carbon nanostructures.

Herein, we report the decatungstate-photocatalyzed acylation of purified semiconducting (7,6)SWCNTs and examine the scope of the functionalization reaction by screening different aldehydes, namely alkyl, aromatic, and organometallic ones, as well as by varying the reaction time. Aldehydes, particularly, as small organic molecules with characteristic spectroscopic fingerprint due to the carbonyl group, bear the major advantage of easy monitoring the chemical transformation and purification of the modified SWCNTs by IR spectroscopy. Furthermore, by performing a series of blank experiments, we were able to provide significant insight into the role of illumination and TBADT as catalyst in the process. Given the mild reaction conditions required, the vast availability of starting materials along with the fact that the catalyst and unreacted aldehydes can be recovered and reused as well as the modified SWCNTs being easily isolated and purified by simple membrane filtration, the developed methodology is also considered validated and ideal from the vantage point of industries.

2. Results and Discussion

Purified semiconducting (7,6)SWCNTs in *ortho*-dichlorobenzene (*o*-DCB)/acetonitrile mixture (85/15 v/v), excess of aldehyde **1a-c** and a catalytic amount of TBADT were irradiated with a 500 W Xenon lamp. The reaction mixture was kept under reduced temperature and inert atmosphere, while alternating sonication/light-irradiation and stirring for 5 h was employed. After that period, the unreacted aldehyde **1a-c** and TBADT catalyst were removed by filtration over PTFE membrane (0.2 μm pore size) and the modified (7,6)SWCNT-based materials **2a-c** (Figure 1a) were obtained as solid by extensive washing with dichloromethane. In more detail, light irradiation generates holes at the HOMO of the complex, transforming W₁₀O₃₂⁻⁴ to W₁₀O₃₂^{-4*} followed by quick relaxation to the wO intermediate. Further, wO has the required oxidative potential to abstract a hydrogen atom from aldehyde **1a-c**, producing the corresponding acyl radical species. Then, the so-formed W₁₀O₃₂⁻⁵ reduces (7,6) SWCNTs, recovering the original W₁₀O₃₂⁻⁴ and activating the latter to quickly capture the acyl radical (Figure 1b). Although we do not have direct proof for the reaction mechanism, it is reasonable to assume that the decatungstate-photocatalyzed acylation of (7,6)SWCNTs follows similar pathway with that occurring with the modification of fullerenes.^[14] Please note that absence of oxygen and accurate control of temperature

were necessary to avoid oxidation and decarboxylation of the **1a-c** aldehyde.^[12,14] This is proved by ¹H NMR spectroscopy, which revealed exclusively the presence of employed aldehyde in the filtrate, proving its stability during the decatungstate-photocatalyzed acylation of (7,6)SWCNTs (Figure S1, Supporting Information). Although NMR spectroscopy is an unambiguous spectroscopic technique to monitor organic transformations in molecules, it cannot be extended to low-dimensional carbon nanomaterials such as SWCNTs. Mainly, this is due to the inhomogeneity of SWCNTs, being a polydisperse mixture composed of nanotubes with different lengths and different diameters that are aggregated in bundles of different size, as well as the irregular and multiple presence of addends onto their skeleton. To overcome this issue, complementary spectroscopic characterization, in both solid-state and solution, was performed, together with thermal analysis and microscopy imaging of the (7,6)SWCNT-based materials **2a-c**.

First, IR as a nondestructive and essential spectroscopic means was employed to identify the presence of covalently added species onto the sidewalls of modified (7,6)SWCNTs. Carbonyl vibrations of starting aldehyde **1a**, **1b**, and **1c**, appearing at 1708, 1677, and 1658 cm⁻¹, respectively, shift to higher energies, once transformed in ketones within acyl functionalized (7,6) SWCNTs **2a**, **2b**, and **2c**, at 1720, 1715, and 1699 cm⁻¹, respectively (Figure S2, Supporting Information). Notably, the intensity of the ketone vibration increases with time of reaction, suggesting higher acylation degree – see for example in Figure 2, the progressive development of the relative IR band for **2b**, after TBADT-photocatalyzed acylation reaction of (7,6)SWCNTs for 1, 2, 3, and 5 h.

Next, Raman spectroscopy was used to monitor alterations occurred at (7,6)SWCNTs sidewalls upon photocatalytic acylation. As a representative example, Raman spectra and maps of **2c** are shown in Figure 3, while the corresponding spectra and maps for materials **2a** and **2b** can be found at the Supporting Information (Figure S3, Supporting Information). We observe in all materials **2a-c** the characteristic RBM (261 cm⁻¹), D (1335 cm⁻¹), G (1560 cm⁻¹), D' (1520 cm⁻¹), D'' (1591 cm⁻¹), and 2D (2633 cm⁻¹) bands.^[22] The G-band is characteristic of in-plane displacement of sp²-carbons, and a red shift of 3.0, 2.0, and 2.5 cm⁻¹ in **2a**, **2b**, and **2c**, respectively, in comparison with that of purified (7,6) SWCNTs, guarantees strong interactions between SWCNTs and the acyl moieties present onto the sidewalls (Figure 3a,b). The D-band is related with disorder on the hexagonal lattice (sp³-carbons) of (7,6)SWCNTs and enhancement of the D/G intensity ratio has been widely employed to justify covalent functionalization.^[23] In our case, the D/G average ratio enhances from 0.4 in purified (7,6)SWCNTs to 1.8, 1.0, and 1.5 in **2a**, **2b**, and **2c**, respectively (Figure 3a). Spatial Raman spectroscopy mapping, calculating the D/G ratio over long distances and multiple locations (100 μm²), ensures a rather homogeneous functionalization in **2a-c**, with absence of impurities (Figure 3c).

The functionalization extent, in terms of acyl groups incorporated onto the sidewalls of (7,6)SWCNTs, is assessed by thermogravimetric analysis performed in N₂ atmosphere. Purified (7,6)SWCNTs are thermally stable, even at temperature higher than 500 °C, under inert conditions. However, in modified (7,6) SWCNTs **2a-c**, the organic addends thermally degrade at that

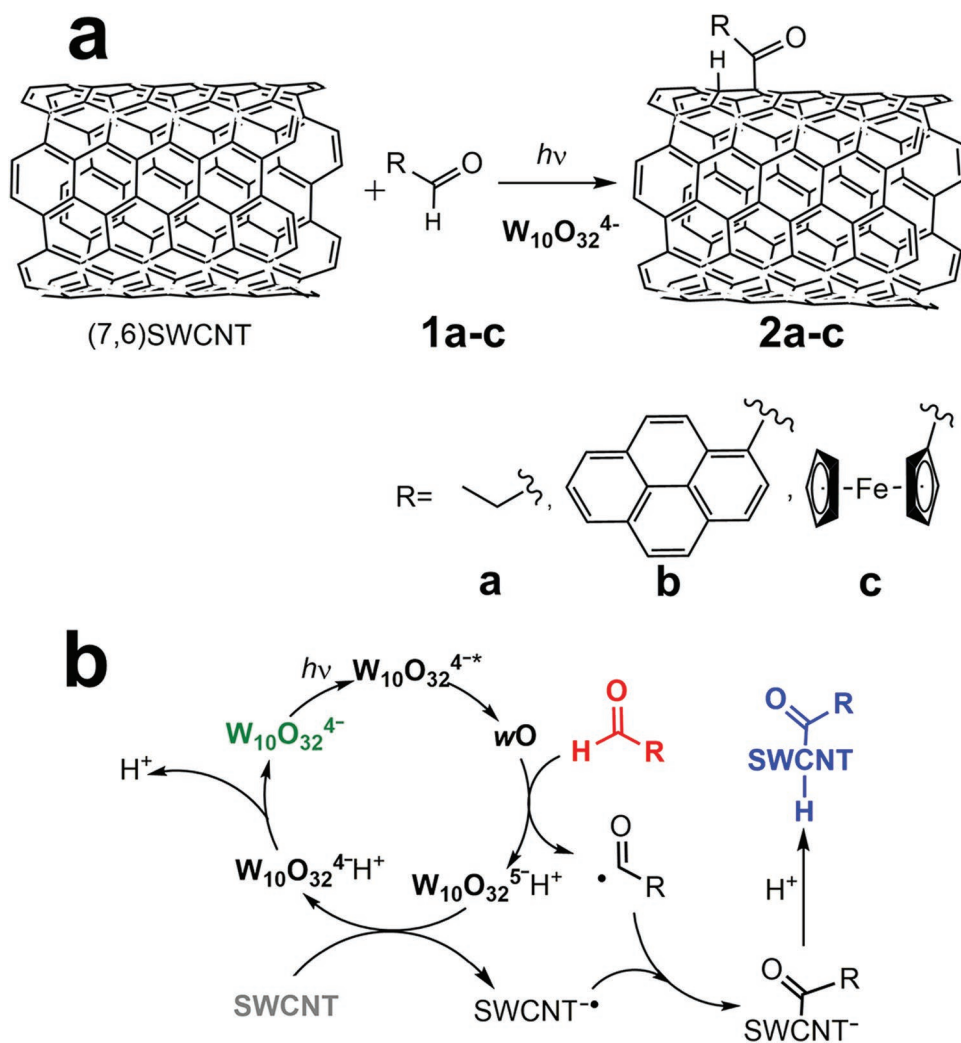


Figure 1. a) Decatungstate-photocatalyzed acylation of (7,6)SWCNTs yielding functionalized materials **2a-c**, and b) mechanism of the catalytic acylation cycle.

temperature (Figure 4). Specifically, the weight loss at 500 °C for **2a**, **2b**, and **2c** is 6%, 1%, and 5%, respectively, which is translated to the presence of 1 acyl moiety, per 83, 1800, and 320 carbon atoms of (7,6)SWCNTs, respectively. For the same photocatalytic acyl functionalization of (7,6)SWCNTs, the difference on the loading in **2a-c** is justified by considering steric effects, e.g., the most sterically demanding reactant, pyrene aldehyde **1b**, results on the least loading in functionalized **2b**, while the smallest propanal **1a** yields modified (7,6)SWCNTs **2a** with the highest loading. Furthermore, increasing the mass amount of the aldehyde enhances the functionalization level. For example, employing quadruple amount of **1a** yields 1 acyl unit per every 25 carbon atoms of (7,6)SWCNTs, according to TGA (Figure S4, Supporting Information).

TEM imaging was employed to visualize the morphology of **2a-c**. All materials show aggregations of several SWCNTs without appreciable differences, ensuring that not only the morphology but also the crystallinity is preserved. Figure 5a shows a representative TEM image of few-aggregated nanotubes of **2c**. Moreover, EDS (Figure 5b) shows a peak at 6.38 keV,

confirming the presence of Fe due to the grafted ferrocene units in **2c**. Similar TEM images for **2a** and **2b** are shown at Figure S5 in the Supporting Information.

At this point, we have full proof for the TBADT-photocatalyzed acylation of (7,6)SWCNTs, evidenced by different spectroscopic, thermal and microscopy imaging techniques. Based on blank experiments, by performing the reaction of (7,6)SWCNTs with aldehydes **1a-c** and in the presence of TBADT but under dark conditions, no acylation takes place. This is evidenced by the absence of IR vibration modes due to acyl groups as well as the absence of the Raman D-band, and importantly the insolubility of the material in any organic solvent. In addition, reaction of (7,6)SWCNTs with aldehydes **1a-c** and light irradiation but without TBADT as catalyst, similarly, does not yield any product. Hence, the catalytic role of TBADT is evident and photoillumination is required for obtaining (7,6)SWCNT-based materials **2a-c**.

Turning our focus in solution spectroscopic examination of the decatungstate-photocatalyzed acylation of (7,6)SWCNTs, pyrene in **1b** is an appropriate marker to follow the success of

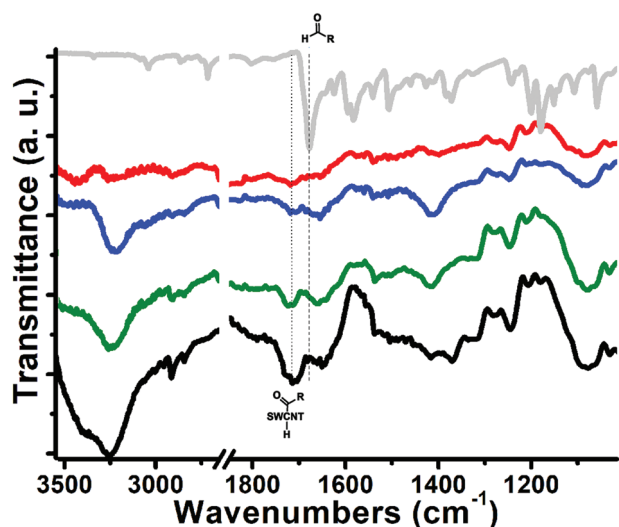


Figure 2. IR spectra of aldehyde **1b** (gray) and functionalized material **2b** obtained after 1 h (red), 2 h (blue), 3 h (green), and 5 h (black) of decatungstate-photocatalyzed acylation of (7,6)SWCNTs. The dotted lines are for guiding the shift of the carbonyl vibration.

the reaction in wet media. Hence, in the UV–vis spectrum of **2b** absorption bands from pyrene are evident at 233, 284, and 368 nm (Figure 6a), on top of the characteristic van Hove singularities of semiconducting (7,6)SWCNTs^[24] S_{22} and S_{11} at 678 and 1158 nm, respectively (the S_{33} at around 375 nm is masked under pyrene absorption). Careful comparison of the UV–vis spectrum of **2b** with that of **1b** and purified (7,6)SWCNTs reveal changes due to electronic ground-state interactions between the two species, e.g., the S_{22} and S_{11} SWCNT-centered bands are red-shifted by 5 and 10 nm, respectively, while the pyrene bands at 235 and 367 nm show a marginal blue shift of 3 and 1 nm, respectively. While this absorbance shift indicates orbital coupling between pyrene and (7,6)SWCNTs in **2b**, the delicate appearance of SWCNTs absorption signatures in the NIR region agrees with a low level of honeycomb disturbance. Moreover, the pyrene unit allows following the decatungstate-photocatalyzed acylation of (7,6)SWCNTs in **2b** via photoluminescence spectroscopy. Hence, the fluorescence emission of pyrene in **2b** at 371 nm, upon 330 nm excitation in dichloromethane (Figure 6b), is found 3 nm red-shifted compared to that of free pyrene employed as reference compound, and highly quenched ($\approx 70\%$ based in samples possessing equal optical concentration at the excitation wavelength). In addition, the fluorescence decay of **2b** was examined and curve-fitted by the dual exponential function, yielding a very short fluorescence lifetime of 55 ps and another longer one of 1.7 ns, with the latter resembling that of free pyrene. Those photophysical findings are in harmony with earlier reports of covalently anchored pyrene units onto carbon nanostructures.^[25–27]

Finally, exploiting the redox properties of ferrocene in **2c**, cyclic voltammetry was employed to further assess the photocatalytic acylation of (7,6)SWCNTs. The measurement was performed in dry benzonitrile under N_2 atmosphere and 0.1 M tetrabutylammonium hexafluorophosphate as electrolyte, with platinum wire as reference and auxiliary electrodes and glassy

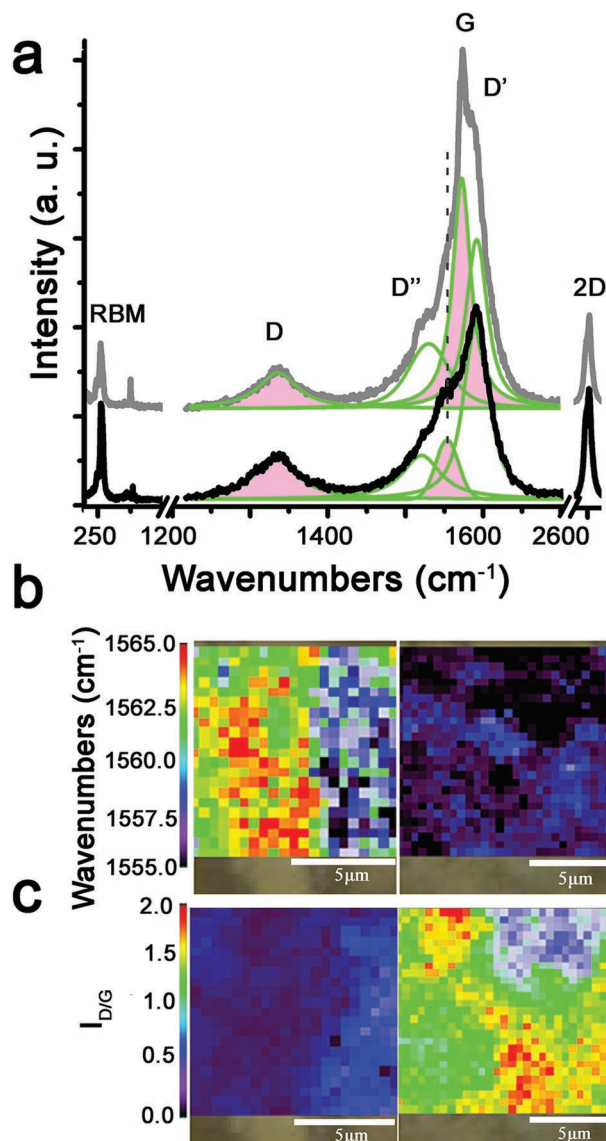


Figure 3. a) Raman (514 nm) spectra of purified (7,6)SWCNTs (gray) and functionalized material **2c** (black); the green lines are the deconvoluted spectra and the dotted line is for guiding the shift of the G-band. Raman (514 nm) spectral maps of b) G-band, and c) intensity ratio $I_{D/G}$ of purified (7,6)SWCNT (left panel) and functionalized material **2c** (right panel).

carbon as working electrode. Thus, **1c** shows an oxidation process due to ferrocene species at 1.26 V, which is found shifted to higher oxidation potential by 90 mV, at 1.35 V, in **2c** (Figure 7). At the reduction path, while purified (7,6)SWCNTs show discrete processes at -0.73 and -1.57 V, in **2c** they are registered at -0.78 and -1.60 V, shifted at lower reduction potential by 50 and 30 mV, respectively. Similar redox shifts were recorded for **2b** (Figure S6, Supporting Information), due to the presence of pyrene. Those redox alterations in **2b** and **2c** not only showcase the corresponding modification of (7,6)SWCNTs framework, but also pinpoint the development of electronic interactions between the electroactive species grafted and (7,6)SWCNTs.

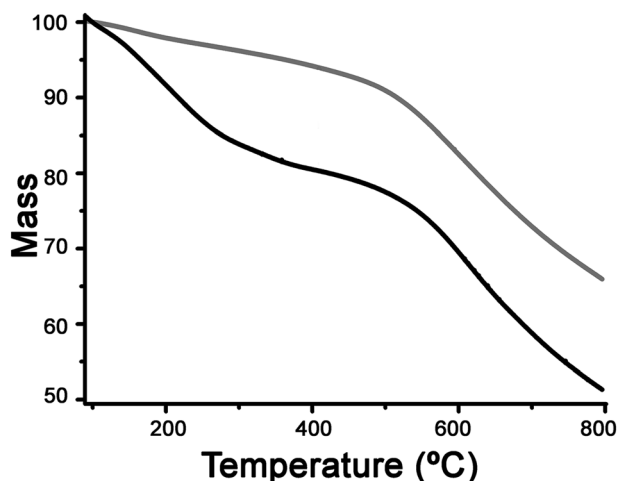


Figure 4. TGA graph of purified (7,6)SWCNT (gray) and functionalized material **2a** (black), obtained under nitrogen.

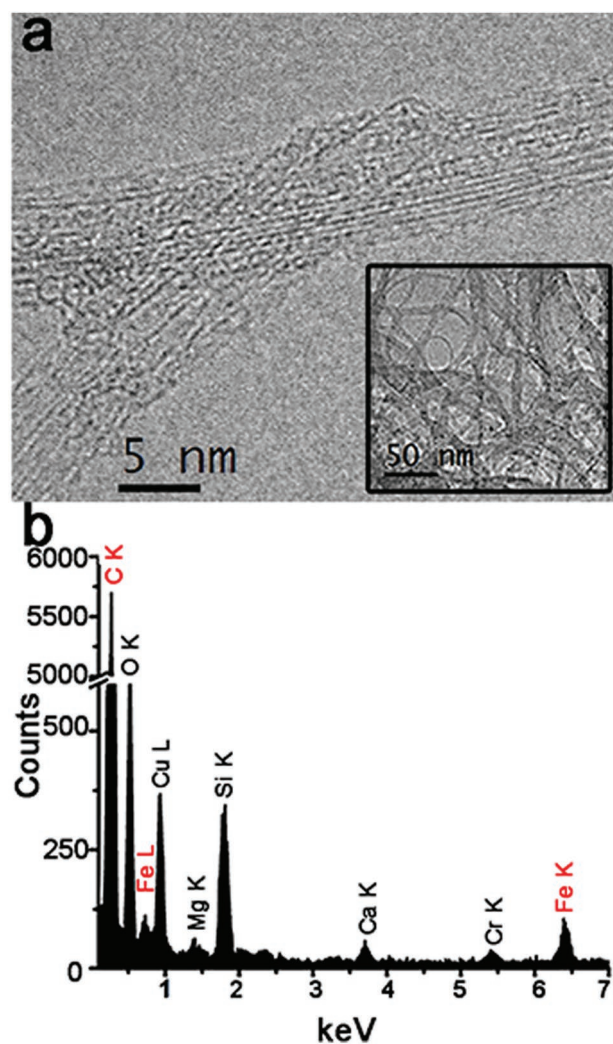


Figure 5. a) High magnification TEM image of functionalized material **2c**. Inset: Low magnification image of **2c**. b) EDS of **2c**. The presence of Cu, Si, and Cr is due to sample holder and grid used for the measurement, while the presence of Mg and Ca are due to impurities from the glass vial.

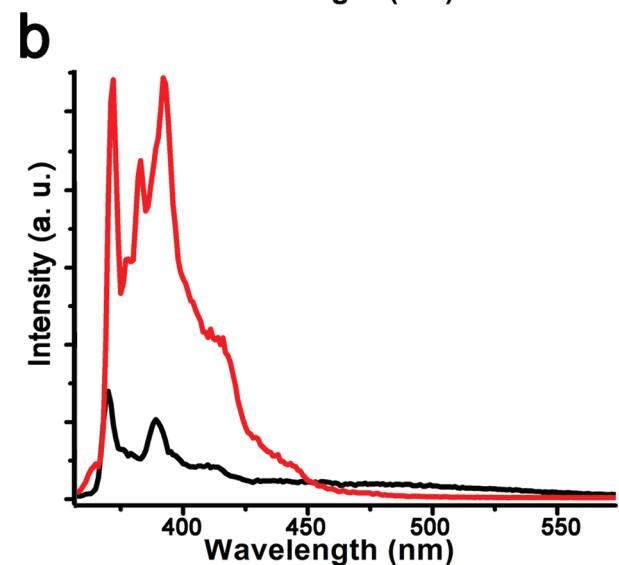
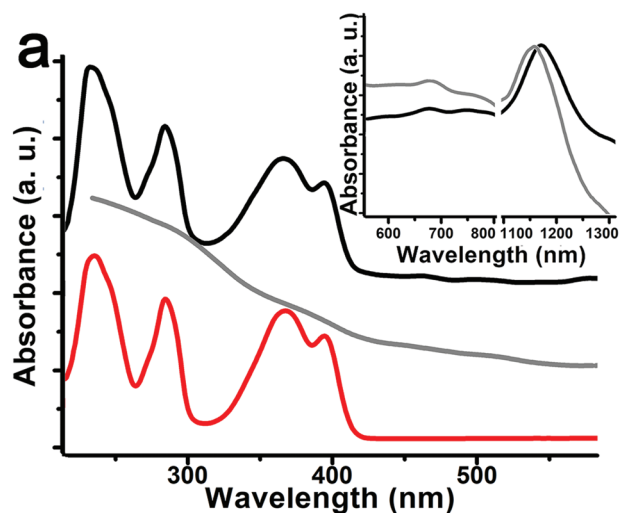


Figure 6. a) UV-vis-NIR spectrum of pyrene derivative **1b** (red), functionalized material **2b** (black), and purified (7,6)SWCNTs (gray), in dichloromethane. Inset: expansion of the NIR region showing characteristic absorbance due to (7,6)SWCNTs, in deuterated aqueous 1% sodium dodecyl benzene sulfonate. b) PL fluorescence emission spectrum of **1b** (red) and **2b** (black), in dichloromethane.

3. Conclusion

The decatungstate-photocatalyzed acylation of semiconducting (7,6)SWCNTs was accomplished. The developed strategy is highly effective as determined by employing a range of aldehydes, e.g., alkyl, aromatic and organometallic. Moreover, it is environmentally friendly, since the catalyst and unreacted aldehydes can be recovered and reused, while the modified SWCNTs can be easily isolated and purified by membrane filtration. This is the first time a straightforward catalytic process for the modification of SWCNTs is realized, providing unambiguous spectroscopic evidence for the modified material, and expands the utility of polyoxometallates in the chemical transformation of SWCNTs. As such, the decatungstate-photocatalyzed acylation of SWCNTs is pioneering and paves the way for a new area of research in low-dimensional nanomaterials. Given the mild

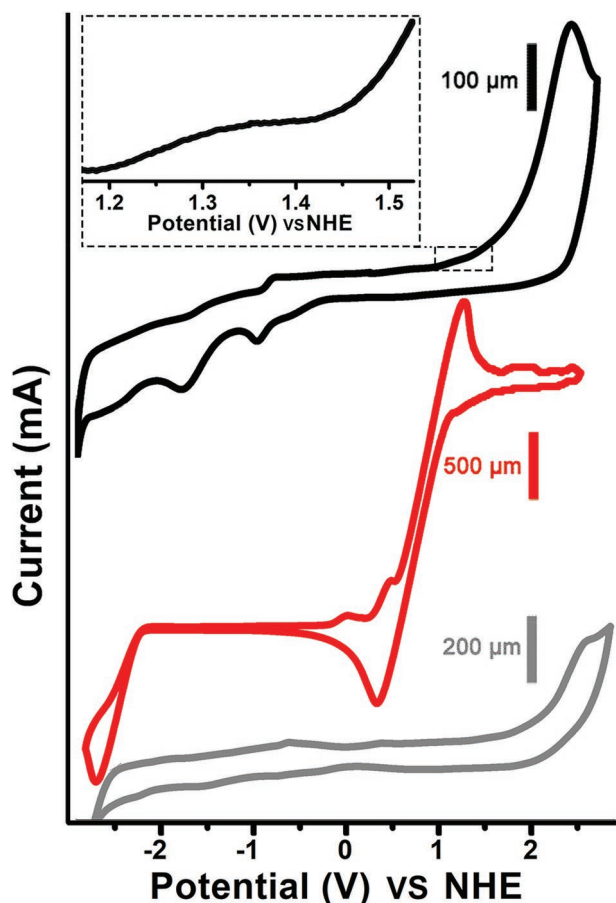


Figure 7. Cyclic voltammetry graph of ferrocene derivative **1c** (red), functionalized material **2c** (black), and purified (7,6)SWCNTs (gray).

reaction conditions required and the vast availability of starting materials, the methodology outlined is also considered ideal from the vantage point of industries.

4. Experimental Section

Purification of (7,6)SWCNTs: Initially, raw (7,6)SWCNTs (150 mg) were refluxed in concentrated HCl (25 mL) for 48 h with occasional sonication. After that period, the reaction mixture was filtered through a PTFE membrane (0.2 μm pore size) and the solid residue was washed with water, methanol, and dichloromethane to obtain purified (7,6)SWCNTs, according to literature procedures.^[28]

Decatungstate-Catalyzed Acylation of (7,6)SWCNTs: Purified (7,6)SWCNTs (20 mg) were dispersed in *o*-DCB/acetonitrile 85:15 (100 mL) and the reaction mixture was degassed under nitrogen. Then a catalytic amount of TBADT (18.5 mg) and the aldehyde substrate **1a-c** (2.7 mmol) were added. The reaction mixture was subsequently irradiated for 5 h with a 500 W Xenon lamp, while maintaining the temperature at 5–10 °C with an ice bath and shortly sonicating the reaction mixture every 30 min to ensure good dispersion. After that period, the reaction mixture was filtered through a PTFE membrane (0.2 μm pore size) and the solid residue was washed with *o*-DCB and dichloromethane to obtain materials **2a-c**.

Supporting Information

Supporting Information is available from the Wiley Online Library or from the author.

Acknowledgements

This project has received funding from the European Union's Horizon 2020 research and innovation programme under the Marie Skłodowska-Curie grant agreement N° 642742. The authors are indebted to Emeritus Professor Michael Orfanopoulos, Department of Chemistry, University of Crete, Greece, for introducing them in the research field of photomediated catalysis with decatungstate complex.

Conflict of Interest

The authors declare no conflict of interest.

Data Availability Statement

The data that support the findings of this study are available from the corresponding author upon reasonable request.

Keywords

acylation, decatungstate, functionalization, photocatalysis, single-walled carbon nanotubes (SWCNTs)

Received: July 18, 2022
Revised: September 18, 2022
Published online: October 19, 2022

- [1] J. Zhang, M. Dai, S. Zhang, M. Dai, P. Zhang, S. Wang, Z. He, *Sol. RRL* **2022**, *6*, 202200243.
- [2] G. Hills, C. Lau, A. Wright, S. Fuller, M. D. Bishop, T. Srimani, P. Kanhaiya, R. Ho, A. Amer, Y. Stein, D. Murphy, A. C. Arvind, M. M. Shulaker, *Nature* **2019**, *572*, 595.
- [3] M. F. L. De Volder, S. H. Tawfick, R. H. Baughman, A. J. Hart, *Science* **2013**, *339*, 535.
- [4] J. C. Charlier, X. Blase, S. Roche, *Rev. Mod. Phys.* **2007**, *79*, 677.
- [5] S. Mallakpour, S. Soltanian, *RSC Adv.* **2016**, *6*, 109916.
- [6] N. Karousis, N. Tagmatarchis, D. Tasis, *Chem. Rev.* **2010**, *110*, 5366.
- [7] A. Hirsch, O. Vostrowsky, *Topics Curr. Chem.* **2005**, *245*, 193.
- [8] M. Tzirakis, I. Lykakis, M. Orfanopoulos, *Chem. Soc. Rev.* **2009**, *38*, 2609.
- [9] C. Tanielian, *Coord. Chem. Rev.* **1998**, *178*, 1165.
- [10] C. Tanielian, R. Seghrouchni, C. Schweitzer, *J. Phys. Chem. A* **2003**, *107*, 1102.
- [11] G. Laudadio, Y. Deng, K. van der Wal, D. Ravelli, M. Nuño, M. Fagnoni, D. Guthrie, Y. Sun, T. Noël, *Science* **2020**, *369*, 92.
- [12] G. da Silva, J. Bozzelli, *J. Phys. Chem. A* **2006**, *110*, 13058.
- [13] M. D. Tzirakis, M. Orfanopoulos, *Org. Lett.* **2008**, *10*, 873.
- [14] M. Tzirakis, M. Orfanopoulos, *J. Am. Chem. Soc.* **2009**, *131*, 4063.
- [15] M. Tzirakis, M. Orfanopoulos, *Angew. Chem., Int. Ed.* **2010**, *49*, 5891.
- [16] M. Tzirakis, M. Alberti, M. Orfanopoulos, *Chem. Commun.* **2010**, *46*, 8228.
- [17] N. Malliaros, I. Kellner, T. Drewello, M. Orfanopoulos, *J. Org. Chem.* **2021**, *86*, 9876.
- [18] X. Zhang, X. Li, *Chin. Chem. Lett.* **2014**, *25*, 501.
- [19] V. de Waele, O. Poizat, M. Fagnoni, A. Bagno, D. Ravelli, *ACS Catal.* **2016**, *6*, 7174.
- [20] N. Murakami, Y. Tango, H. Miyake, T. Tajima, Y. Nishina, W. Kurashige, Y. Negishi, Y. Takaguchi, *Sci. Rep.* **2017**, *7*, 43445.
- [21] D. Ravelli, S. Montanaro, C. Tomasi, P. Galinetto, E. Quartarone, D. Merli, P. Mustarelli, M. Fagnoni, *ChemPlusChem* **2012**, *77*, 210.

- [22] Y. Choi, K. Min, M. Jeong, *J. Nanomater.* **2013**, 615915.
- [23] S. Deng, Y. Zhang, A. Brozena, M. Mayes, P. Banerjee, W. Chiou, G. Rubloff, G. Schatz, Y. Wang, *Nat. Commun.* **2011**, 2, 1384.
- [24] C. Shearer, L. Yu, A. Blanch, M. Zheng, G. Andersson, J. Shapter, *J. Phys. Chem. C* **2019**, 123, 26683.
- [25] A. Sandanayaka, G. Pagona, J. Fan, N. Tagmatarchis, M. Yudasaka, S. Iijima, Y. Araki, O. Ito, *J. Mater. Chem.* **2007**, 17, 2540.
- [26] T. Umeyama, J. Baek, Y. Sato, K. Suenaga, F. Abou-Chahine, N. Tkachenko, H. Lemmetyinen, H. Imahori, *Nat. Comm.* **2015**, 6, 8732.
- [27] M. Álvaro, P. Atienzar, J. Bourdelande, H. García, *Chem. Phys. Lett.* **2004**, 384, 119.
- [28] E. Edwards, E. Antunes, E. Botelno, M. Baldan, E. Corat, *Appl. Surf. Sci.* **2011**, 258, 641.